VORTICITY IN THE MAGNETOSPHERIC PLASMA AND ITS SIGNATURES IN THE AURORA DYNAMICS

MIKHAIL I. PUDOVKIN

Institute of Physics, St. Petersburg University, St. Petersburg, Petrodvorets, 198904, Russia

AKE STEEN and URBAN BRÄNDSTRÖM

Swedish Institute of Space Physics, Box 812, S-981 28 Kiruna, Sweden

Abstract. A review of both the theoretical and experimental data connected with the vorticity in the magnetospheric plasma and on its signatures in the auroral dynamics is presented. It is shown that the observed characteristics of the motion of auroral forms allow one to determine the distribution of the electric field and field-aligned currents in the magnetosphere; the shape of auroral vortices and their power spectra carry information on the nature of the MHD instabilities responsible for the excitation of the observed turbulence.

The complex of experimental data necessary for a confident description of the electrodynamic state of the magnetosphere is discussed.

1. Introduction

For a long time it has been recognized that observations of aurorae provide us with an abundance and variety of information on the physical processes which develop in the magnetospheric plasma. In particular, the characteristics of optical spectra of aurorae permit one to determine the nature of precipitated particles (whether they are electrons or protons), and on their energy spectra (Chamberlain, 1961). On the other hand, observations of energy spectra of auroral electrons provide evidence for the existence of electrostatic double layers on auroral magnetic field lines, and allow one to estimate the location and main parameters of those layers (Evans, 1974, 1975). The global distribution of auroral arcs permit one to trace the large-scale convection of the magnetospheric plasma (Davis, 1962), and to calculate the intensity of the convection electric field in the magnetosphere (Pudovkin et al., 1968).

One of the most general and at the same time greatly informative characteristics of aurorae is the vorticity observed in their geometric structure and in their motion. Over the last two decades, many publications have appeared which are devoted to experimental and theoretical consideration of the magnetospheric plasma vorticity. It has been shown that observed characteristics of auroral vorticity (the characteristic shape of vortices, the sense of rotation, their power spectra) allow one to determine the parameters of the ambient plasma, the nature of the vorticity source, and the physical mechanisms exciting the turbulence.

On the other hand, the characteristics of plasma turbulence may be of great importance in transport processes in the collisionless magnetospheric plasma, such
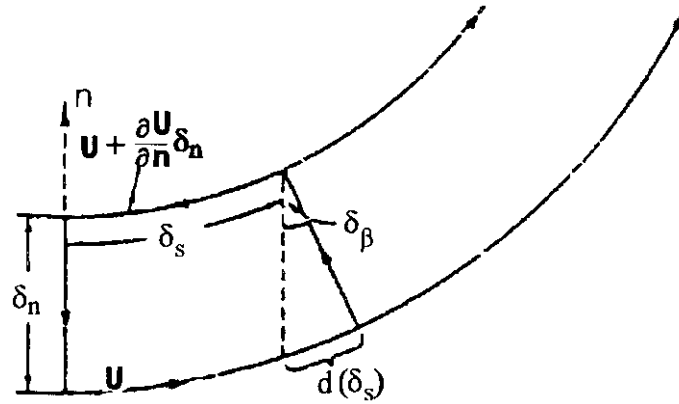
Figure 1. Calculation of the vorticity (after Holton, 1992).

as the turbulent viscosity, diffusion coefficient, electric and thermal plasma conductivity, etc. (Liperovsky and Pudovkin, 1983).

In this paper we shall review papers devoted to consideration of the fluid and plasma vorticity and their application to auroral dynamics, with the aim of presenting a consistent account of basic ideas on magnetospheric plasma vorticity, on the excitation of the latter, on its ionospheric signatures, and on the information which the observations of auroral vorticity provide on magnetospheric processes.

2. Vorticity Equation

Vorticity (ζ) is the measure of rotation in a fluid:

$$\zeta = \operatorname{rot} \mathbf{u} , \tag{1}$$

where $\mathbf{u}$ is the fluid velocity. The physical meaning of the vorticity may be illustrated by the following consideration (Holton, 1992).

Let us consider two-dimensional motion of a fluid (Figure 1) and compute the circulation (C) of the velocity along the contour shown in Figure 1:

$$\delta C = u[\delta s + d(\delta s)] - \left(u + \frac{\partial u \delta n}{\partial n} \right) \delta s = \left(-\frac{\partial u}{\partial n} + u \frac{\delta \beta}{\delta s} \right) \delta n \, \delta s , \tag{2}$$

where n is the normal to the stream lines and $\delta \beta$ is the angular change in the flow velocity direction over the distance δs. Then the value of ζ equals:

$$\zeta = \lim_{\delta n, \delta s \to 0} \frac{\delta C}{\delta n \, \delta s} = -\frac{\partial u}{\partial n} + \frac{u}{R_s} , \tag{3}$$

where R_s is the radius of curvature of the streamlines. One can see from Equation (3) that the vorticity is the sum of two parts: (1) the rate of change of the fluid velocity normal to the flow direction, $-\delta u/\delta n$, called the shear vorticity; and (2) the rotation of the velocity vector along a stream line u/R_s, called the curvature vorticity. Thus, and this may be important for interpretation of auroral configurations, the vorticity may exist even within a flow with rectilinear stream lines, or be absent within a flow with curved stream lines (see Section 4).

The change of the vorticity along a stream line is described by the vorticity equation which may be obtained from the equation of motion:

$$\frac{d\mathbf{u}}{dt} = \frac{\partial \mathbf{u}}{\partial t} + (\mathbf{u} \cdot \nabla)\mathbf{u} = \frac{1}{\rho}\mathbf{F} \; . \tag{4}$$

Taking the curl of Equation (4), one obtains (Batchelor, 1970):

$$\frac{\partial \boldsymbol{\zeta}}{\partial t} + (\mathbf{u} \cdot \nabla)\boldsymbol{\zeta} + \boldsymbol{\zeta} \, \mathrm{div}\mathbf{u} - (\boldsymbol{\zeta} \cdot \nabla)\mathbf{u} = \frac{1}{\rho}\mathrm{rot}\,\mathbf{F} - \frac{\nabla\rho}{\rho^2} \times \mathbf{F} \; ; \tag{5}$$

in deriving Equation (5), we have taken into account that $(\mathbf{u} \cdot \nabla)\mathbf{u} = \frac{1}{2}\nabla(u^2) - \mathbf{u} \times \mathrm{rot}\,\mathbf{u}$; and $\mathrm{rot}\,[\mathbf{a} \times \mathbf{b}] = (\mathbf{b} \cdot \nabla)\mathbf{a} - \mathbf{b}\,\mathrm{div}\,\mathbf{a} - (\mathbf{a} \cdot \nabla)\mathbf{b} + \mathbf{a}\,\mathrm{div}\,\mathbf{b}$.

In a 2D flow (due to the high field-aligned conductivity of the magnetospheric plasma, this approximation is valid in many problems concerned with magnetospheric convection), $(\boldsymbol{\zeta} \cdot \nabla)\mathbf{u} = 0$, and Equation (5) reduces to

$$\frac{d\boldsymbol{\zeta}}{dt} + \boldsymbol{\zeta} \, \mathrm{Div}\,\mathbf{u} = \frac{1}{\rho}\mathrm{rot}\,\mathbf{F} - \frac{\nabla\rho}{\rho^2} \times \mathbf{F} \; , \tag{5a}$$

where $\mathrm{Div}\,\mathbf{u}$ is the 2D divergence of $\mathbf{u}$.

This is the basic equation describing the behaviour of vorticity in a 2D-flow, and we shall consider below some applications of this equation in connection with magnetospheric plasma convection.

3. Conservation of the Potential Vorticity

Thus, we shall restrict the consideration to a 2D model where the stationary magnetic field in Z-direction and $T_e \gg T_i$. In this case, electron distribution function obey the Boltzmann formula, and relatively cold protons may be considered as a fluid which motion may be described by the equation (Hasegawa and Sato, 1989):

$$\frac{d\mathbf{u}}{dt} = -\frac{e}{m_i}\nabla\varphi + \Omega_i[\mathbf{u} \times \mathbf{e}_z] - \frac{1}{nm_i}\nabla p_i \; , \tag{6}$$

where $\Omega = eB/m_i c$ is the ion gyrofrequency and p_i is the ion pressure, and Equation (5a) reduces to:

$$\frac{d\boldsymbol{\zeta}}{dt} + \boldsymbol{\zeta} \cdot \text{Div}\,\mathbf{u} = -\Omega_i \mathbf{e}_z\,\text{Div}\,\mathbf{u} + \frac{1}{n^2 m_i}\nabla n \times \nabla p_i - (u \cdot \nabla)\Omega_i \mathbf{e}_z \,. \qquad (7)$$

With the aid of the continuity equation:

$$\frac{\partial n}{\partial t} + \text{div}(n\mathbf{u}) = 0 \,, \qquad (8)$$

one obtains from Equation (7):

$$\frac{d(\boldsymbol{\zeta} + \boldsymbol{\Omega}_i)}{dt} - \frac{1}{n}(\boldsymbol{\zeta} + \Omega_i \mathbf{e}_z)\frac{dn}{dt} = \frac{1}{n^2 m_i}\nabla n \times \nabla p_i = \frac{1}{nm_i}\nabla n \times \nabla \Theta_i \,, \quad (9)$$

where $\Theta_i = kT_i$. Equation (9) may be considered as a modification of the Bjerkness theorem, well-known in meteorology (see Fleagle and Businger, 1980, p. 174); according to this theorem, vorticity is excited when constant pressure (or constant temperature) surfaces do not coincide with constant density surfaces (baroclinic flow in meteorology).

In the case of cold ions, or when ∇n is parallel to $\nabla \Theta_i$, the right-hand side of Equation (9) equals zero, and it may be rewritten as:

$$\frac{d}{dt}\ln\frac{\boldsymbol{\zeta} + \Omega_i}{n} = 0 \quad \text{or} \quad \frac{d}{dt}\frac{\boldsymbol{\zeta} + \Omega_i}{n} = 0 \,, \qquad (10)$$

which is the equation of vorticity conservation for a compressible fluid with a transverse magnetic field (Hasegawa and Sato, 1989, Section 2.9).

Petviashvili (1977), Hasegawa and Sato (1989), Laedke and Spatschek (1986), Spatschek and Laedke (1986) pointed out that Equation (10) is similar to the barotropic (Rossby) potential vorticity equation:

$$\frac{d}{dt}\left(\frac{\boldsymbol{\zeta} + \mathbf{f}}{h}\right) = 0 \,, \qquad (11)$$

where $f = 2\Omega_E \sin \Phi$ is the Coriolis parameter, Ω_E is the Earth's rotation velocity, h is the fluid depth, and Φ is the latitude of the point under consideration (Holton, 1992).

One can see that the value of the potential vorticity $(\boldsymbol{\zeta} + \boldsymbol{\Omega})/n$ is conserved along the stream lines and may be therefore used to identify or tag plasma parcels (Fleagle and Businger, 1980).

In the simplest case of an incompressible plasma and homogeneous, time-independent magnetic field equation (11) reduces to

$$\frac{d\boldsymbol{\zeta}}{dt} = 0 \,. \qquad (12)$$

However, and this is important for magnetospheric physics, for slow vortex motions, the vorticity is approximately conserved not only along stream lines, but also, as we shall show below, along magnetic field lines. As a result, vorticity is transferred from the magnetosphere to the ionosphere, and may be observed there in the dynamics of the ionospheric plasma and in the motion of auroral forms, thereby embodying Akasofu's idea on the ionosphere to be the screen of a huge picture tube-magnetosphere (Akasofu, 1966). What exactly information on the state and parameters of the magnetospheric plasma may be obtained from corresponding observations, is discussed below.

Taking into account the fact that the two-dimensional velocity of an incompressible plasma can be expressed by a stream function Ψ such that:

$$\mathbf{u} = \nabla\Psi \times \mathbf{e}_z \quad \text{and} \quad \boldsymbol{\zeta} = -\nabla^2\Psi \cdot \mathbf{e}_z \, , \tag{13}$$

Equation (12) may be rewritten as

$$\frac{\partial}{\partial t}\nabla^2\Psi + ([\nabla\Psi \times \mathbf{e}_z]\nabla)\nabla^2\Psi = 0 \, . \tag{14}$$

This equation is typical for vortex-type situations: it contains a twisting nonlinearity, and localized solutions in Ψ result in a vortex-type motion for $\mathbf{u}$ (Spatschek and Laedke, 1986).

Equation (14) plays an important role in the physics of the magnetospheric plasma, where the frozen-in property of the plasma and magnetic field results in an electric field drift of the plasma:

$$\mathbf{u}_{\mathrm{E}} = -c\frac{\nabla\varphi \times \mathbf{e}_B}{B} \, , \tag{15}$$

where φ is the electrostatic potential, and $\mathbf{e}_B$ is the unit vector along the $\mathbf{B}$-field. One can see that in the case of a homogeneous magnetic field, Equation (15) is similar to Equation (13) with

$$\Psi = -\frac{c}{B}\varphi \, , \quad \text{and} \quad \boldsymbol{\zeta} = \frac{c}{B}\nabla^2\varphi\mathbf{e}_B \, , \tag{16}$$

so that Equation (14) reduces to:

$$\frac{\partial}{\partial t}\nabla^2\varphi - \frac{c}{B}[(\nabla\varphi \times \mathbf{e}_B) \cdot \nabla)\nabla^2\varphi = 0 \, . \tag{17}$$

Spatschek and Laedke (1986) have shown that in the case of an inhomogeneous magnetic field the electric drift velocity (Equation (15)) may be written in a strongly analogous form to Equation (13). Indeed, normalizing φ by T_e/e, where T_e is the electron temperature, the perpendicular length by the thermal ion Larmor radius ρ_s, and $\mathbf{u}$ by $u_{T,e}$, one has:
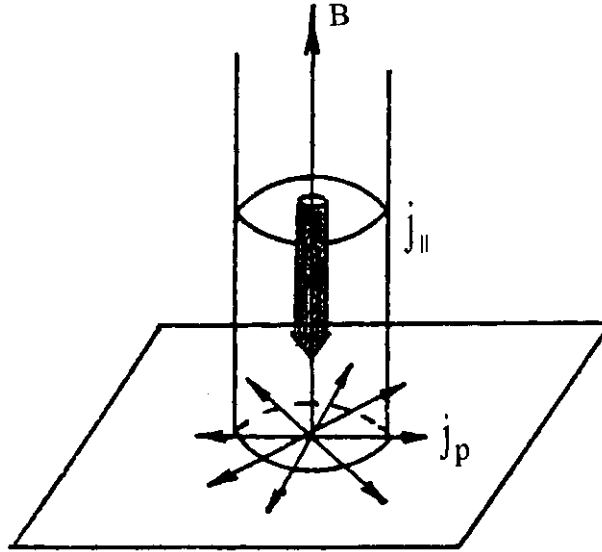
Figure 2. Scheme of the magnetospheric plasma vorticity transfer to the ionosphere.

$$\tilde{\mathbf{u}} = -\tilde{\nabla}\tilde{\varphi} \times \mathbf{e}_B \ , \tag{18}$$

where the tilde denotes normalized variables.

4. Quasi-Steady-State Circulation of the Magnetospheric Plasma

The equations of vorticity conservation (Equation (10) or Equation (14)) are valid when the sources and sinks of the vorticity, described by the right-hand side of Equation (5), are absent or balance each other. At the same time, as we have said above, the vorticity associated with the convective flow of magnetospheric plasma is transferred to the ionosphere, where some dissipative effects do exist. Thus, the steady-state circulation of magnetospheric plasma may be realized only when the dissipative effects are balanced by some processes producing vorticity. This situation may be illustrated by considering the following elementary example. Let the magnetic field be homogeneous and directed along the Z-axis (see Figure 2), and let the plasma (supposed to be homogeneous) rotate around one of the magnetic field lines, on which an electric charge exists; further on we shall suppose that this charge exists only inside a field-aligned cylinder with radius r_0, so that the linear charge equals $Q = \pi r_0^2 q$, where q is the charge density, supposed to be homogeneous inside the cylinder. Then the electric field intensity equals

$$E_r(r) = 2\pi q r \quad \text{inside the cylinder} \ ,$$

and

$$E_r(r) = \frac{2Q}{r} \qquad \text{outside the cylinder}, \tag{19}$$

and the plasma motion velocity is determined by Equation (15) so that

$$u_\varphi = -c\frac{2\pi q r}{B} \quad \text{for} \quad r \le r_0,$$

$$u_\varphi = -c\frac{2Q}{rB} \quad \text{for} \quad r \ge r_0, \tag{20}$$

As is seen from Equation (20), in the region outside the charged cylinder the plasma vorticity $\zeta_z = r^{-1}\,\partial/\partial r(ru_\varphi)$ equals 0 since the curvature vorticity is compensated for by the shear vorticity:

$$\frac{\partial u_\varphi}{\partial r} = -\frac{u_\varphi}{r} = c\frac{2\pi r_0^2 q}{r^2 B}\,.$$

At the same time, the non-zero circulation of the velocity along any stream line around the cylinder shows that somewhere inside the region limited by that streamline, plasma vorticity has to exist. Indeed, inside the cylinder, $\zeta = -(c/B)4\pi q = (c/B)\nabla^2\varphi$, which agrees with Equation (16b).

We have supposed the magnetic field to be homogeneous in the above example. However, in the real magnetosphere it is dipole-like and hence greatly inhomogeneous. In this connection we shall now assume the field lines to converge toward the ionosphere so that the radius of the cylinder shown in the figure equals r_m in the magnetosphere and r_i in the ionosphere, and $r_i < r_m$. Because of the very high conductivity of the magnetospheric plasma, magnetic field lines may be considered as equipotentials. In this case, the transverse electric field at the top of the ionosphere equals $E_i = E_m(r_m/r_i)$, where E_m is the magnetospheric electric field, and, according to Equation (19), the electric charge density in the ionosphere is $q_i = q_m(r_m/r_i)^2$. The magnetic field intensity also increases towards the ionosphere so that $B_i = B_m(r_m/r_i)^2$, and therefore the plasma motion vorticity in the ionosphere given by Equation (16b) is equal to $\zeta_i = -(c/B_i)4\pi q_i = (-c/B_m)4\pi q_m = \zeta_m$. Thus, the magnetospheric plasma vorticity is conserved along the magnetic field lines and hence is transferred to the ionosphere without any significant changes.

At the same time, one has to bear in mind that it takes for an Alfvénic wave to propagate from the plasma sheet in the magnetotail to the polar ionosphere about 1–2 minutes. Correspondingly, shortly living or rapidly changing vortices cannot be considered as quasi-steady-state phenomena and are not directly projected into the ionosphere.

However, existence of the conductive ionosphere results in appearance of Pedersen currents spreading from the cylinder axis, and this suggests for $\operatorname{div}\mathbf{j} = 0$ existence of field-aligned current $j_\parallel = -\operatorname{div}\mathbf{J}_\perp$, where $\mathbf{J}_\perp$ is the height-integrated

ionospheric current intensity. Taking into account that $\mathbf{J}_\perp = \Sigma_p \mathbf{E}_\perp$, where Σ_p is height-integrated Pedersen conductivity of the ionosphere, one obtains in the case of homogeneous Σ_p:

$$j_\| = -\Sigma_p \operatorname{div} E = -4\pi \Sigma_p q_i \ ,$$

and correspondingly

$$\zeta_i = -\frac{c}{B_i} 4\pi q_i = \frac{c}{B_i \Sigma_p} j_\| \ .$$

Thus, vorticity of the ionospheric plasma motion may procede in a steady-state regime only in the case when field-aligned currents exist, which agrees with results by Southwood and Kivelson (1993).

The intensity of field-aligned currents in the magnetospheric plasma may be obtained from the continuity equation:

$$\frac{\partial j_\|}{\partial z} = -\operatorname{Div} \mathbf{j}_m \ ,$$

or

$$j_\| = -\operatorname{Div} J_m \ ,$$

where J_m is the height-integrated transverse current density; on the other hand, the intensity of the transverse current equals

$$\mathbf{j}_m = c\frac{\mathbf{F} \times \mathbf{B}}{B^2} \ ,$$

and in the case of a homogeneous magnetic ield:

$$\operatorname{Div} \mathbf{j}_m = \frac{c}{B} \operatorname{rot}_z \mathbf{F} \ .$$

Thus, to maintain a steady-state vorticity in the magnetospheric plasma motion, the existence of a vortical force in the magnetosphere (or in the ionosphere) is needed, which agrees with Equation (5).

In the real magnetosphere, the situation is much more complicated: the magnetic field and plasma density are inhomogeneous, magnetic field lines are curved, and the frozen-in conditions may be violated, especially in the case of small-scale or rapidly developing vorticity. However, the vorticity characteristics discussed above are valid even in this case, at least qualitatively: vorticity of the magnetospheric plasma convection is transferred to the ionosphere by field-aligned currents, that is by means of Alfvén waves (Dungey, 1958), and foci of plasma vortices are associated with the existence of regions of space charge ($\nabla^2 \varphi \neq 0$).

Table I
Energy spectral distribution for various forms of turbulence

Wind shear	Viscous dissipation	$F = \dfrac{3}{\sqrt{\pi}} \dfrac{R}{(\partial u / \partial z)} k^{-1}$
	Thermal instability	$F = \frac{1}{3}(\partial U / \partial z)^2 k^{-3}$
No shear	Viscous dissipation	$F = \dfrac{\pi}{6}(R/\eta^2)^2 k^{-7}$
	Thermal instability	$F = \left(\dfrac{32}{9\pi}\right)^{1/3} R^{2/3} k^{-5/3}$
	Nonlinear wave amplification	$F = (\text{const.})\omega_B^2 k^{-3}$

The equations discussed above describe excitation and evolution of relatively large-scale and regular vorticity, all the characteristics of which may be calculated when the initial and boundary conditions are given. However, the flow within those primary vortices may be (and usually is) unstable with respect to development of plasma (or fluid) instabilities of various kinds, which results in appearance of small-scale secondary vortices, or turbulence in the flow.

5. Turbulent Vorticity

Haas (1993) points out that 'it is very useful to describe a turbulent proces into motions which occur on various length scale, because the different scales play different roles in the dynamics. This is generally referred to as eddies of different sizes. On the smaller sizes, individual eddies cannot be identified, and small eddies simply means short range coherence. On the larger scale, however, characteristic features of the motion can be identified'. In this section we shall consider the excitation of those small-scale, turbulent vortices. We shall not be interested in features of individual vortices, but mainly in their statistical characteristics such as the stages of development, the energy spectral distributions, etc. This approach to the problem is determined by the fact that statistical and, in particular, spectral characteristics of the turbulence give us ample information on the mechanism of the turbulence excitation, and thereby, on the state of the magnetospheric plasma in the source regions. Indeed, as is seen in Table I, adopted from the book by Beer (1974), various forms of turbulence are characterized by quite different energy spectra $F(k)$, where k is the wave number. In particular, one can see that the classical Kolmogoroff spectrum $F \sim k^{-5/3}$ is a rather special case, and more generally the spectrum exponent varies from -1 to -7.

The results from Beer are obtained for turbulence in atmospheric motion, and it is interesting to study this problem in connection with the magnetospheric plasma turbulence.
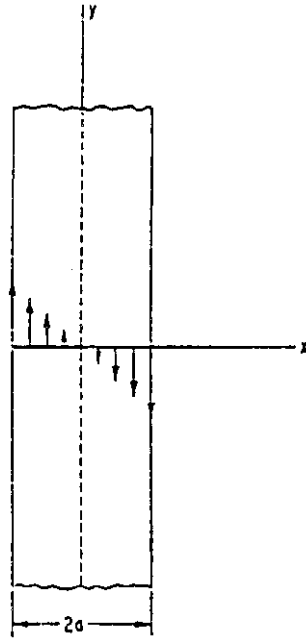
Figure 3. Flat charge sheet showing the distribution of crossed-field drift velocity vectors for electrons within the sheet (after Webster and Hallinan, 1973).

Now we shall consider some special cases of turbulence excitation in the magnetospheric plasma. As one of the most widespread types of turbulence in the magnetospheric plasma is the one associated with drift waves, we shall first of all consider this kind of wave instability.

Drift wave instability.   The drift wave is a local wave which propagates in the direction of the diamagnetic, electric or some other drift velocity in an inhomogeneous plasma. Qualitatively, the development of the drift wave instability in 2D-charge sheets and in current sheets has been considered by Webster and Hallinan (1973), and we shall briefly reproduce their analysis. Let the negative space charge exist in the form of a flat sheet which extends without limit in the Y- and Z-directions and has a thickness $2a$ in the X-direction (Figure 3). Then the electric field equals

$$E_x = -2\pi q x \; ; \tag{21}$$

the magnetic field (B_0) is supposed to be homogeneous and directed along the $(-Z)$ axis. The electron cross field drift velocity $\mathbf{u}$ given by Equation (15) is shown in the figure by arrows; one can see that the electron motion is characterized by a distinct shear of the velocity; at the same time, the net flow (determined by the mean velocity of particles obtained by averaging $\mathbf{u}$ across the layer) equals zero.

Let us suppose now that there appears a small sinusoidal disturbance of the sheet (Figure 4); then the symmetry of the electron velocity across the sheet is
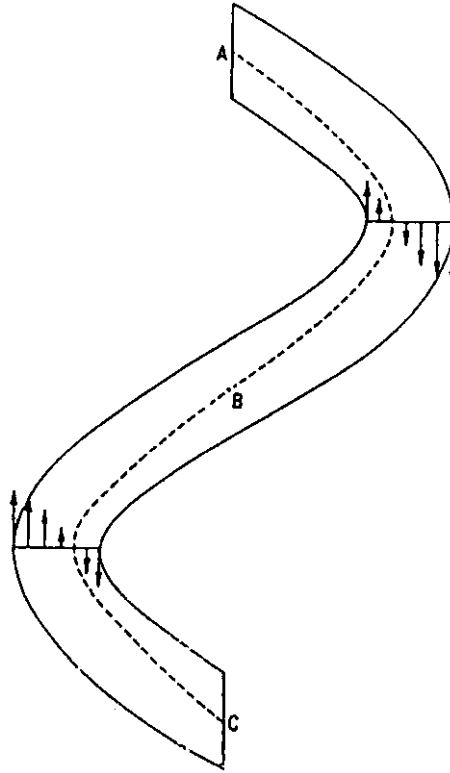
Figure 4. Sinusoidal charge sheet showing the distribution of crossed-field drift-velocity vectors for electrons within the sheet. The magnetic field is pointing away from the viewer (after Webster and Hallinan, 1973).

violated, and a net flow appears from points A and C to point B. This results in a charge concentration at point B, which in turn disturbs the particle motion in such a manner that the point B becomes the centre of a vortex, the arms of which move in a direction so as to increase the ripple amplitude (see Figure 5). The sense of rotation of the arms around a vortex depends upon the sign of the charge and the direction of the magnetic field.

According to Webster and Hallinan (1973) the growth time of the charge-sheet instability is equal to

$$\tau_{ch} = \frac{B_0}{\pi q} \frac{\lambda}{d} \, ,$$

where λ is the wavelength of the disturbance and d is the thickness of the sheet; the most probable wavelength to develop is $\lambda \approx 7.8d$, thus
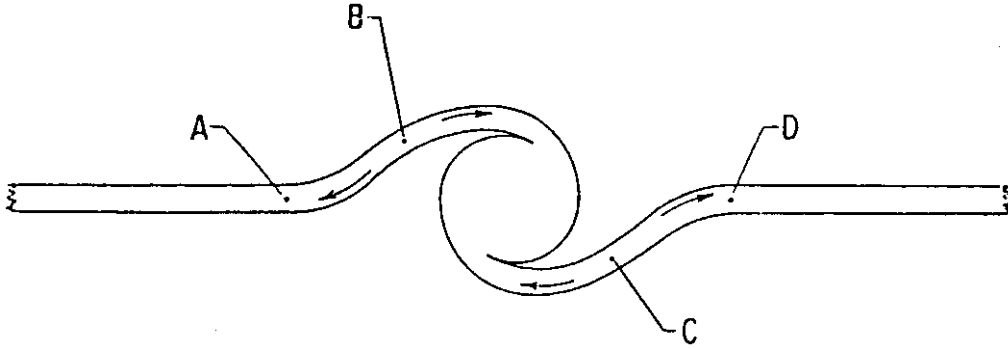
$$\tau_{ch} = 7.8 \frac{B_0}{\pi q} \, ,$$

Figure 5. Single vortex in a flat charge sheet. The magnetic field points away from the viewer (after Webster and Hallinan, 1973).

which is close to the time required for a charge do drift once around a cylinder of uniform charge density. Drift wave instability associated with a shear of $\mathbf{E} \times \mathbf{B}$ drift velocity was considered in more detail by Miura and Sato (1978). These authors have shown that the power spectrum of the excited disturbance may be represented by a power of the form $\sim k^{-4}$, which differs significantly from the Kolmogoroff spectrum.

Following Webster and Hallinan (1973) let us consider now the current sheet instability. The plasma forming the sheet is supposed to be electrically neutral ($q = 0$), and current-carrying particles are moving along the magnetic field lines with a velocity v. The field-aligned current produces a transverse magnetic field B_T ($B_T \ll B_0$), which results in the appearance of a transverse velocity component $v_T = v(B_T/B_0)$, and when the current density within the sheet is homogeneous,

$$B_T = \frac{2\pi j x}{c} \quad \text{and} \quad v_T = v\frac{2\pi j}{cB_0}x \; . \tag{22}$$

One can see from Equation (22) that the distribution of the transverse velocity v_T across the current sheet is described by the same expression as in the case of the charge sheet. Then, if once more we suppose that there appears some sinusoidal disturbance in the current sheet as is shown in Figure 4, this results in the concentration of field-aligned currents at point B, and the particles will stream around B at the speed

$$v_t = \frac{v}{B_0}\frac{2j \, dS}{r} \; , \tag{23}$$

where dS is the cross section of the cylinder; Equation (23) is of the same form as the drift velocity of particles streaming around a charge cylinder (see Equation (20)). Thus, just as in the case of a charged sheet, a small sinusoidal disturbance of the current sheet geometry will result in appearance of vortices, the amplitude of which will grow with time.

Concerning the sense of the vortex rotation, one can see that in the case when current-carrying particles are electrons, moving parallel to B_0 (see Figure 3), the field-aligned currents are directed along the positive Z-axis, B_T and v_T are in the opposite direction to the arrows in the figure, and the arms are rotating around the vortex centre in the counter-clockwise direction.

If the direction of the particle flow is reversed, the tangential component B_T is also reversed. However, since the flow is changed from parallel to antiparallel to B_0, the tangential motion is now antiparallel to the tangential field and hence is still in the initial direction. Thus, the direction of particle motion does not affect the direction of arm rotation.

This dependence for both the charge and current sheets is summarized in Table II, after Webster and Hallinan (1973).

Table II

Appearance of a vortex produced by various instabilities (for a magnetic field pointing toward the viewer)

Instability	Charged particles	Appearance of vortex
Charge sheet	Electrons	
	Protons	
Current sheet	Electrons	
	Protons	

The mechanism of formation of auroral spirals was later considered by Hallinan (1976). The author arrives at the conclusion that in a magnetic field under the proper circumstances there are two vector quantities each of which can play a role similar to that of the velocity in an compressible sheared fluid. These quantities are velocity of the frozen-in field lines in the presence of a divergent electric field, and the magnetic field itself in the presence of field-aligned currents which fulfill the role of vorticity. Analysis of the configuration of the magnetic field in the vicinity of a current sheet has shown that auroral spirals correspond to an equilibrium configuration of the distorted current sheet rather than to a current sheet instability.

In this connection we have to note that a transfer from a homogeneous current sheet to a curled one is associated with a re-distribution of the magnetospheric plasma pressure, and for the equation of motion is not considered by the author, the process of a new equilibrium configuration is not quite clear.

A more elaborate model of the drift wave instability was presented by Hasegawa and Sato (1984) and Laedke and Spatschek (1986). Following their analysis, we shall consider drift wave excitation in a plasma consisting of cold ions and hot
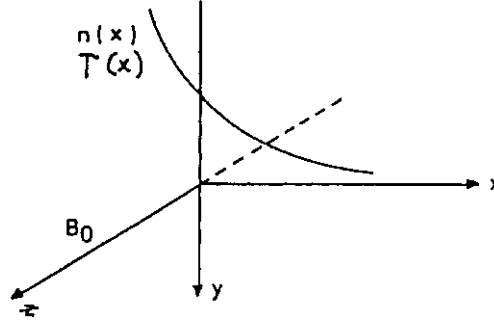
Figure 6. Investigation of a drift wave in a uniform magnetic field.

electrons $T_i \ll T_e$ in a slab geometry with a homogeneous magnetic field $\mathbf{B} = B\mathbf{e}_z$, and with the density and temperature gradients in the x-direction (Figure 6). Besides, we shall consider the disturbed electric field to be a self-consistent field associated with the wave propagation, and the number density of the cold ions will be supposed to be the same as of electrons (quasi-neutrality requirement) and hence to obey the Boltzmann distribution for electrons:

$$n_i \approx n_e = n_0(x) \exp(e\varphi/\Theta_e) \approx n_0(x) \left(1 + e\varphi/\Theta_e\right) , \tag{24}$$

where $\Theta_e = kT_e$.

Equation (6) results in (Karlson, 1962; Laedke and Spatschek, 1986):

$$\mathbf{v}_i = \mathbf{v}_i^0 - \frac{c^2 m_i}{eB^2} \left[\left(\left(\frac{\partial}{\partial t} + \mathbf{v}_i^0 \cdot \nabla \right) \mathbf{E} \right) \times \mathbf{e}_z \right] =$$

$$- \frac{c(\nabla\varphi \times \mathbf{e}_z)}{B} - \frac{c}{B\Omega_i} \frac{\partial}{\partial t} \nabla\varphi + \frac{c^2}{B^2\Omega_i}([\nabla\varphi \times \mathbf{e}_z] \cdot \nabla)\nabla\varphi ; \tag{25}$$

here $\mathbf{v}_i^0 = (c/B) \left[\mathbf{E} \times \mathbf{e}_z \right]$ is the drift velocity in the zeroth approximation.

Then, having inserted Equations (24) and (25) into the continuity equation (8), one obtains:

$$\frac{n_0 e}{\Theta_e} \frac{\partial\varphi}{\partial t} - \frac{n_0 c}{B\Omega_i} \frac{\partial}{\partial t}\nabla^2\varphi + \frac{n_0 c^2}{\Omega_i B^2}([\nabla\varphi \times \mathbf{e}_z] \cdot \nabla)\nabla^2\varphi -$$

$$- \frac{c}{B}([\nabla\varphi \times \mathbf{e}_z] \cdot \nabla)n_0 - \frac{c}{B}([\nabla\varphi \times \mathbf{e}_z] \cdot \nabla) \left(\frac{e\varphi}{\Theta e} \right) = 0 , \tag{26}$$

or, taking into account that $\nabla\varphi$ is orthogonal to $[\nabla\varphi \times \mathbf{e}_z]$, so that $[\nabla\varphi \times \mathbf{e}_z]\nabla\varphi = 0$,

$$\frac{\partial}{\partial t}(\varphi - \rho_L^2 \nabla^2 \varphi) + \frac{c}{B}\rho_L^2([\nabla\varphi \times \mathbf{e}_z]\cdot\nabla)\nabla^2\varphi - \frac{c}{B}\frac{\Theta_e}{n_0 e}([\nabla\varphi \times \mathbf{e}_z]\cdot\nabla)n_0 +$$

$$+ \frac{c\varphi}{Bn_0}([\nabla\varphi \times e_z]\nabla)\ln\Theta_e = 0 \,, \tag{26a}$$

where

$$\rho_L^2 = \frac{c\Theta_e}{eB\Omega_i} = \frac{\Theta_e}{m_i\Omega_i^2} \,.$$

It is seen that Equation (26) contains two nonlinear terms: the Petviashvili term $([\nabla\varphi \times \mathbf{e}_z]\cdot\nabla)(\varphi/\Theta_e)$ which originates from the plasma electric drift in an inhomogeneous temperature system (Petviashvili, 1977), and the Hasegawa–Mima term $([\nabla\varphi \times \mathbf{e}_z]\cdot\nabla)\nabla^2\varphi$ caused by the nonlinear ion polarization drift. Yu and Lisak (1986) point out that both nonlinear terms appearing in Equation (26) are in the form of Poisson brackets defined by $\{f, g\} = (\partial f/\partial x)(\partial g/\partial y) - (\partial f/\partial y)(\partial g/\partial x)$, indicating that two-dimensional effects are essential; this property is crucial for the existence of a vortex solution.

The nature of Equation (26) and the characteristics of the vorticity described by it depend on which of the two nonlinear terms is predominant. Thus, if the temperature gradient is small or $\Theta_e(x) \approx$ const., the last term on the left-hand side of Equation (26a) may be neglected, and it reduces to:

$$\frac{\partial}{\partial t}(\varphi - \rho_L^2 \nabla^2 \varphi) + \frac{c}{B}\left\{[\nabla\varphi \times e_z]\cdot\nabla(\rho_L^2\nabla^2\varphi - \frac{\Theta_e}{e}\ln(n_0))\right\} = 0 \,, \tag{27}$$

which coincides with the Hasegawa–Mima equation.

In the case of strong temperature inhomogeneities, the second term on the left-hand side of Equation (26a) may be neglected, and one obtains:

$$\frac{\partial}{\partial t}(\varphi - \rho_L^2 \nabla^2 \varphi) - \frac{c}{B}\frac{\Theta_e}{n_0 e}([\nabla\varphi \times e_z]\cdot\nabla)n_0 +$$

$$+ \frac{c\varphi}{Bn_0}([\nabla\varphi \times \mathbf{e}_z]\nabla)\ln\Theta_e = 0 \,, \tag{28}$$

which is analogous to the Petviashvili equation.

Hasegawa and Sato (1986) have considered excitation of drift waves in an isothermal plasma, that is in a situation described by Equation (27). To consider a mode localized in the inhomogeneous region, we shall suppose an exponential spatial profile for the density $n_0(x)$:

$$n_0(x) \sim \exp(-Kx) \,; \tag{29}$$

where $K = 1/L_n$, L_n being the density scale length; it is this density profile which provides the source of free energy for the instability (Haas, 1993).

Besides, we shall consider one-dimensional waves in the form:

$$\varphi = \varphi_k e^{i(k_y y - \omega t)} \, . \tag{30}$$

Then, having substituted Equations (29) and (30) into Equation (27), one obtains:

$$\omega(1 + \rho_L^2 k_y^2) - \frac{c}{B} \frac{\Theta_e}{e} K k_y = 0 \, , \tag{31}$$

or

$$\omega = \frac{\omega_e^*}{1 + \rho_L^2 k_y^2} \, , \tag{32}$$

where $\omega_e^* = (cK\Theta_e/eB)k_y = v_D k_y$ is the electron drift frequency and $v_D = cK\Theta_e/eB$ is the electron diamagnetic drift velocity due to the electron pressure gradient: $v_D = -c\nabla p \times \mathbf{e}_B / n_0 eB$. As is seen from Equation (32), the drift frequency ω^* depends on the value of K, i.e., on the free energy available for instability, and in a homogeneous plasma ($K \to 0$) tends to zero.

As we have seen above, the value of $\nabla^2 \varphi$ determines the plasma vorticity, and, hence, the electrostatic drift wave is a vortex mode. In the one-dimensional flat wave approximation considered above, surfaces of constant $\nabla^2 \varphi$ are planes $Y - v_D t = \text{const.}$, and the vorticity is a shear vorticity, so that no plasma circulation vortices are formed. A much more interesting situation takes place in a two-dimensional model associated with the appearance of closed circulation vortices. Thus, Laedke and Spatschek (1986) have shown that in the case of strong temperature inhomogeneities, the vorticity equation (28) has a solution in the form of unipolar vortices. In contrast to this, in the density gradient case, the vorticity excitation is described by Equation (27) which has a solution in the form of dipolar vortices (so-called modons). Thus, the structure of the observed vorticity allows one to determine the mechanism of excitation of the latter as well as the characteristics of the magnetospheric plasma in the source region.

A three-dimensional model of the MHD-instability of a current layer associated with an oblique Alfvén wave, with the dispersive effects of electron inertia and a reflecting ionosphere taken into account, was developed by Seyler (1990) in order to study the nonlinear plasma dynamics of small-scale arcs. For this purpose the equation of motion (4) with $\mathbf{F} = -\nabla p + c^{-1} j \times \mathbf{B}$:

$$m_i n \left(\frac{\partial \mathbf{u}}{\partial t} + (\mathbf{u} \cdot \nabla)\mathbf{u} \right) = -\nabla p + \frac{1}{c}\mathbf{j} \times \mathbf{B} \tag{33}$$

was augmented by Ohm's law (Rossi and Olbert, 1970) for a collisionless plasma:

$$E + \frac{1}{c}\mathbf{u} \times \mathbf{B} = \frac{m_e}{ne^2} \left[\frac{\partial \mathbf{j}}{\partial t} + \nabla \cdot (\mathbf{uj} + \mathbf{ju}) \right] + \frac{1}{cne}\mathbf{j} \times \mathbf{B} - \frac{1}{2ne}\nabla p \, , \tag{34}$$

where $p = n(\Theta_i + \Theta_e)$ and $\mathbf{ab}$ is the tensor product of the two vectors (i.e., the dyad), and by the Maxwell equations:

$$\mathrm{rot}\mathbf{E} = -\frac{1}{c}\frac{\partial \mathbf{B}}{\partial t} \,, \tag{35}$$

$$\mathrm{rot}\mathbf{B} = \frac{4\pi}{c}\mathbf{j} \,. \tag{36}$$

The magnetic field is supposed to consist of a quasi-stationary external field $\mathbf{B}_0 = B_0\mathbf{e}_z$ and a perturbed transverse one: $\mathbf{B}_1 = \mathbf{e}_z \times \nabla\alpha$, where α is the perturbed flux function, so that

$$\mathbf{B} = B_0\mathbf{e}_z + \mathbf{e}_z \times \nabla_\perp\alpha \,, \tag{37}$$

$$\nabla^2\alpha = \frac{4\pi}{c}j_z \,. \tag{38}$$

A simplified model is derived from a systematic expansion in the small parameter $\epsilon \equiv \omega/\Omega_i \ll 1$.

To first order in ϵ the perpendicular part of Ohm's law (34) reduces to the frozen-in condition (15).

The vorticity equation for the problem under consideration may be obtained as usual by taking the z-component of the curl of the equation of motion (33) with $\mathbf{u}$ given by Equation (15):

$$\left(\frac{\partial}{\partial t} + \frac{c}{B}[\mathbf{e}_z \times \nabla_\perp\varphi] \cdot \nabla_\perp\right)\nabla_\perp^2\varphi =$$

$$\frac{B_0}{4\pi m_i n_0 c}\left(B_0\frac{\partial}{\partial z} + [\mathbf{e}_z \times \nabla_\perp\alpha] \cdot \nabla_\perp\right)\nabla_\perp^2\alpha \,. \tag{39}$$

On the other hand, from the induction equation (35) with $\mathbf{E}$ given by Equation (34) and $\mathbf{B}$ by Equation (37) one has to order ϵ^2:

$$\left(\frac{\partial}{\partial t} + \frac{c}{B}[\mathbf{e}_z \times \nabla_\perp\varphi] \cdot \nabla_\perp\right)\left(\alpha - \frac{c^2 m_e}{4\pi n e^2}\nabla_\perp^2\alpha\right) = c\frac{\partial\varphi}{\partial z} \,. \tag{40}$$

Equations (39) and (40) are two equations for two scalar fields φ and α, and they determine the temporal and spatial behaviour of the magnetic and electric fields for given initial and boundary conditions.

First of all, we shall derive the dispersion relation for the propagation of kinetic Alfvén waves. Having supposed all variables to be of the form $\sim e^{-i(\omega t - k_z z - \mathbf{k}_\perp \mathbf{r}_\perp)}$, we may rewrite Equations (39) and (40) as

$$\omega\varphi = \frac{-B_0^2}{4\pi n_0 m_i c}k_z\alpha \,, \qquad \omega\left(1 + \frac{c^2 m_e}{4\pi n e^2}k_\perp^2\right)\alpha = -ck_z\varphi \,, \tag{41}$$

and therefrom:

$$\omega^2 = \frac{k_z^2 v_{\mathrm{A}}^2}{1 + k_\perp^2 \lambda^2} ,\tag{42}$$

where $\lambda^2 = c^2 m_e / 4\pi n_0 e^2 = c^2 / \Pi_e^2$ is the collisionless plasma skin depth. One can see from Equation (42) that small transverse scale waves propagate slower than larger-scale waves; for $k_\perp \to 0$, $\omega^2 \to k_z^2 v_{\mathrm{A}}^2$, and the wave propagates along the magnetic field lines at the Alfvén speed.

The model given by the system of Equations (39)–(40) admits a non-trivial two-dimensional steady-state solution if the source of the Alfvén wave is moving normal to the plane of the current sheet and if certain magnetospheric and ionospheric boundary conditions are imposed.

Thus, let us consider a two-dimensional current sheet (with $\partial / \partial y = 0$) moving along the x-axis with a velocity v_d. We transform to the frame of the drifting sheet (or of the drifting source of the Alfvén wave); then the velocity term $c/B[e_z \times \nabla_\perp \varphi]$ which is present on the left-hand side of Equation (39) and Equation (40) has to be replaced by $\mathbf{v}_1 = c/B[\mathbf{e}_z \times \nabla_\perp \varphi] - v_d$, and those equations may be rewritten for a 2D-problem ($\partial / \partial y = 0$) and for steady-state conditions ($\partial / \partial t = 0$) as:

$$\frac{\partial^2}{\partial x^2} \left(v_d \frac{\partial \varphi}{\partial x} + \frac{B_0^2}{4\pi n_0 m_i c} \frac{\partial \alpha}{\partial z} \right) = 0 \tag{43a}$$

and

$$v_d \frac{\partial}{\partial x} \left(\alpha - \lambda^2 \frac{\partial^2 \alpha}{\partial x^2} \right) + c \frac{\partial \varphi}{\partial z} = 0 .\tag{43b}$$

In deriving Equation (43) we have taken into account that in the two-dimensional case $[e_z \times \nabla_\perp] = 0$.

From Equation (43a) one obtains: $\partial \alpha / \partial z = -(v_d c / v_{\mathrm{A}}^2)(\partial \varphi / \partial x) + Ax + B$; for convenience, we shall suppose that $A = B = 0$; taking the derivative of Equation (43b) with respect to z, and substituting the value off $\partial \alpha / \partial z$, one obtains:

$$v_d^2 \frac{\partial^2}{\partial x^2} \left(\varphi - \lambda^2 \frac{\partial^2 \varphi}{\partial x^2} \right) = v_{\mathrm{A}}^2 \frac{\partial^2 \varphi}{\partial z^2} .\tag{44}$$

The solution of Equation (44) may be expressed in terms of a Fourier series: $\varphi(x, z) = \Sigma_{k=-\infty}^\infty \varphi_k \exp\{i(k_x x + k_z z)\}$; having inserted this expression for $\varphi(x, z)$ into Equation (44), one obtains: $k_z = k_x \cdot (v_d / v_{\mathrm{A}})(1 + \lambda^2 k_x^2)^{1/2}$, and the general solution for $\varphi(x, z)$ may be written as:

$$\varphi(\tilde{x}, \tilde{z}) = \sum_{k_x = -\infty}^\infty \varphi_k \exp\{i k_x (\tilde{x} \pm \delta (1 + \lambda^2 k_x^2)^{1/2} \tilde{z}\} ,\tag{45}$$

where the tilde denotes, as earlier, dimensionless variables: $\tilde{x} = 2\pi x/L_x$ and $\tilde{z} = 2\pi z/L_z$; L_x and L_z are some characteristic lengths (e.g., dimensions of the box in the case of numerical simulations), and $\delta = v_d L_z/v_\mathrm{A} L_x$ is the drift parameter; harmonic amplitudes φ_k are to be found from the boundary conditions at the magnetopause and the ionosphere.

The magnetic flux function α may be obtained from Equation (43a) with the use of Equation (45):

$$\alpha(\tilde{x}, \tilde{z}) = \mp \sum_{k_x=-\infty}^{\infty} \frac{\varphi_k}{(1 + \lambda^2 k_x^2)^{1/2}} \exp\{ik_x[\tilde{x} + 2\pi\delta(1 + \lambda^2 k_x^2)^{1/2}\tilde{z}]\} \ . \tag{46}$$

The field-aligned electric field intensity may be obtained from Equation (34). For the z-component of $\mathbf{E}$, the leading terms are of order ϵ^2, and

$$E_z = -\frac{1}{c}[\mathbf{e}_z \times \nabla_\perp \varphi] \cdot \nabla_\perp \alpha + \lambda^2 \left(\frac{\partial}{\partial t} + ([\mathbf{e}_z \times \nabla_\perp \varphi] \cdot \nabla_\perp\right) \nabla_\perp^2 \alpha \ . \tag{47}$$

Once again having substituted $[e_z \times \nabla\varphi]$ by $([e_z \times \nabla\varphi] - (B/c)v_d)$, and taking into account that $[\mathbf{e}_z \times \mathbf{k}_x] \cdot \mathbf{k}_x = 0$, one obtains for a steady-state solution

$$E_\parallel = -\frac{\lambda^2 B v_d}{c}\frac{\partial^3 \alpha}{\partial x^3} \tag{48}$$

and the field-aligned current intensity is given by Equation (38).

As is seen from Equation (48), a parallel electric field exists only when $v_d \neq 0$, that is when the arc, or more accurately the source of field-aligned currents, is drifting with respect to the ambient plasma.

An example of the steady-state solution given by Equations (45) and (46) is presented in Figure 7, after Seyler (1990). In constructing this figure, the z-coordinate was transformed into the q-coordinate ($\mathrm{d}z = v_\mathrm{A}\,\mathrm{d}q$), to take into account variations of the ionospheric plasma density n_0 and hence of the Alfvén velocity v_A with altitude. One can see from the figure that the current contours close lower in the ionosphere than the potential contours, since the Pedersen currents closing the $j_\parallel$ require ion-neutral collisions and higher plasma density. Besides, one can see that the positive field-aligned electric field occurs in the region of negative $\partial j_\parallel/\partial x$.

However, the two-dimensional current system is unstable with respect to the development of transverse disturbances. To study the time-dependent 3D-problem, Equations (39) and (40) were replaced by the complete equations which contain time-dependent, collisional and dissipative terms:
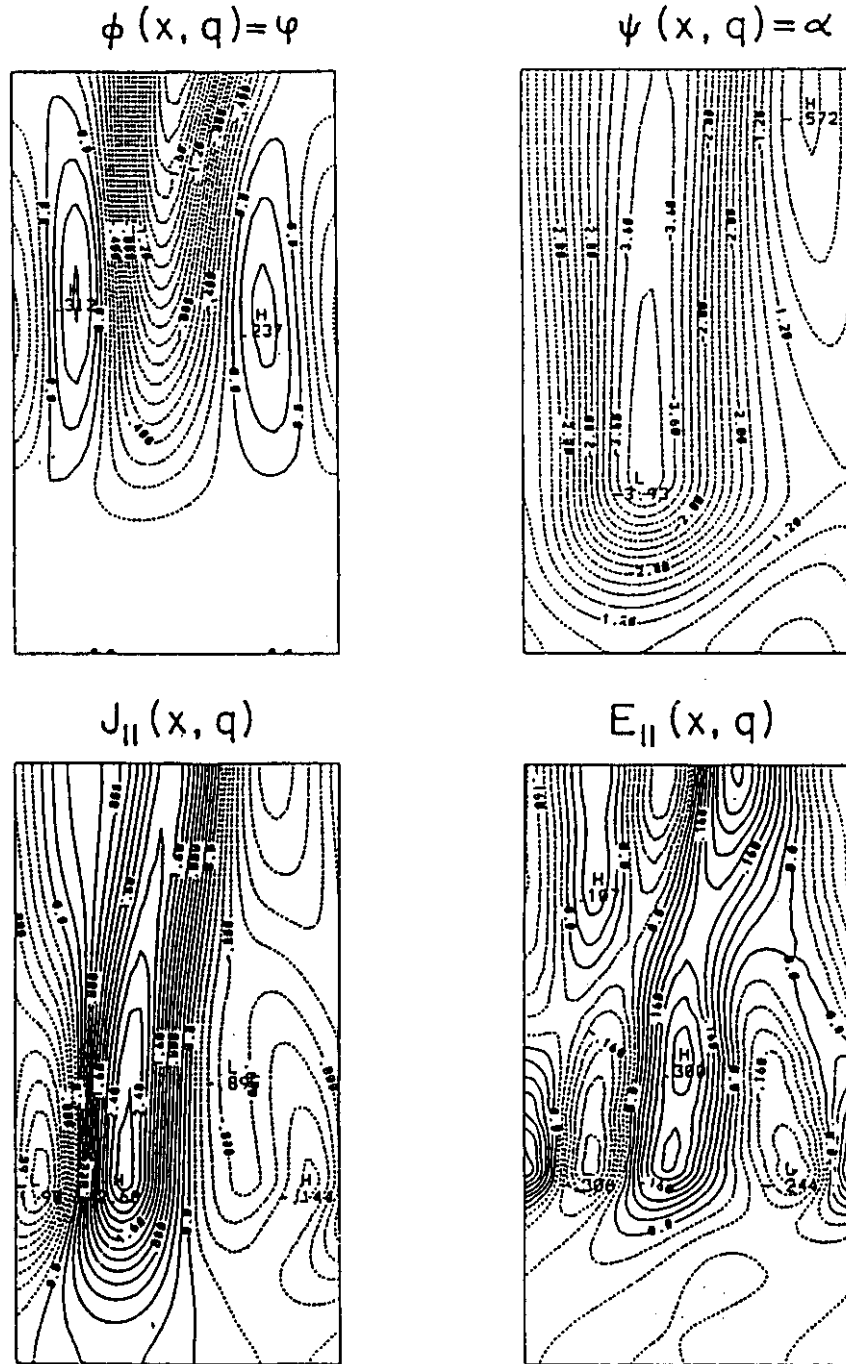
$$\phi (x, q) = \varphi \qquad \psi (x, q) = \alpha$$

$$J_{||} (x, q) \qquad E_{||} (x, q)$$

Figure 7. Contour plots in the $x - q$ plane (starting at upper left and going clockwise) of the electrostatic potential (φ), the magnetic flux function (α), the parallel electric field (E_z) and the parallel electric current density ($j_{||}$) for the V-shock steady-state arc (after Seyler, 1990).
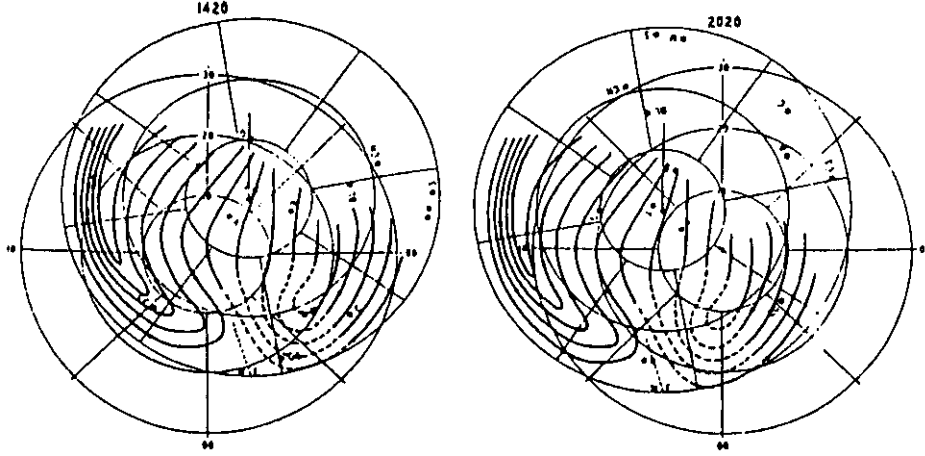
Figure 8. Global distribution of auroral arcs at various moments of universal time (after Davis, 1962).

$$\left(\frac{\partial}{\partial t} - v_d \frac{\partial}{\partial x} + \frac{c}{B}[\mathbf{e}_z \times \nabla_\perp \varphi] \cdot \nabla_\perp + \nu(q)\right)\nabla_\perp^2 \varphi =$$

$$= \left(\frac{n_0(q_0)}{n_0(q)}\right)^{1/2} \frac{B_0}{4\pi n_0 m_i c}\left(B_0 \frac{\partial}{\partial q} + \left(\frac{n_0(q_0)}{n_0(q)}\right)^{1/2}[\mathbf{e}_z \times \nabla_\perp \alpha] \cdot \nabla_\perp\right)\nabla_\perp^2 \alpha; \tag{49}$$

$$\left(\frac{\partial}{\partial t} - v_d \frac{\partial}{\partial x} + \frac{c}{B}[\mathbf{e}_z \times \nabla_\perp \varphi] \cdot \nabla_\perp\right)(\alpha - \lambda^2 \nabla_\perp^2 \alpha) =$$

$$= c \left(\frac{n_0(q)}{n_0(q_0)}\right)^{1/2} \frac{\partial \varphi}{\partial q} + \eta(q)\frac{c}{B_0}, \tag{50}$$

where η is the resistive diffusion coefficient.

Besides, a small perturbation of the form $\sin(k_n y - \omega t)$ has been introduced. Numerical integration of the system of Equations (49) and (50) has shown that:

(a) Two-dimensional steady-state arcs are unstable to three-dimensional disturbances. The arcs evolve through a combination of collisionless tearing and shear flow, with stronger driving field-aligned current resulting in more rapid three-dimensional evolution.

(b) The transverse electric field spectrum of a three-dimensionally evolving arc appears to approach a $k^{-5/3}$ power law as time progresses.

We have considered some of the basic mechanisms of plasma turbulence excitation. In recent years, many papers have been published devoted to the study of various MHD and kinetic plasma instabilities in association with the dynamics of aurorae. However, a detailed analysis of these studies is outside the scope of this paper, the main purpose of which is to demonstrate what kind of information on

the magnetospheric plasma physics may be supplied by observations of the auroral dynamics, and in particular, of the auroral vorticity. In this connection we shall only briefly review some recent papers on the subject.

Haas (1993) has studied excitation of drift waves in the slab geometry considered above (see Figure 6) with a homogeneous magnetic field in a 2D-model with warm ions and with a kinematic ion viscosity $\mu = 3T_i\nu_{ii}/10m_i\Omega_i^2$ (where ν_{ii} is the ion collision frequency) taken into account. It was shown that in the case under consideration the energy spectrum of the excited waves is $E_k \sim k^{-3}$ instead of the Kolmogoroff–Kraichnan spectrum $E_k \sim k^{-5/3}$.

Scott (1990) investigated the excitation of collisional drift waves in a slab geometry with a sheared magnetic field:

$$\mathbf{B} = B_0 \left(\mathbf{e}_z + \frac{x}{L_s}\mathbf{e}_y \right) , \tag{51}$$

where L_s is the shear length, and he found that this model is linearly stable; at the same time, it is unstable with respect to nonlinear (finite amplitude) disturbances.

Hasegawa (1970) and Hasegawa and Sato (1986) studied the development of the current-sheet kink instability that is caused by the tendency of the magnetic field lines, which are bent by the current, to become straight. A threshold intensity was found of the field-aligned current intensity corresponding to the development of the kink instability.

Rostoker and Samson (1984), Rajaram et al. (1986), Connors and Rostoker (1993), and Walker (1981) have studied the Kelvin–Helmholtz instability in shear layers at the interface between the low-latitude boundary layer (LLBL) and the central plasma sheet (CPS) or at the boundary separating the sunward convective flow in the plasma sheet and the region closer to the Earth where flow is slow and due to corotation.

In the next section of the paper we shall briefly review papers concerned with experimental data on the auroral vorticity and the explanation of the latter from the viewpoint of the magnetospheric plasma turbulence models.

6. Experimental Data on Vorticity in Aurora

As the brief review of present-day ideas concerning the vorticity in the magnetized plasma shows, in the magnetosphere we can expect excitation of a series of various plasma instabilities associated with the development of vorticity in the plasma motion and with the appearance of some curl-like structures in auroral forms. Indeed, direct observations of aurorae show that they display a great variety of curled, folded and rotating structures.

On magnetically quiet days, vorticity of the large-scale magnetospheric convection is determined by the boundary conditions at the magnetopause and in the ionosphere, and really proceeds in a quasi-steady-state regime, or slowly varies in
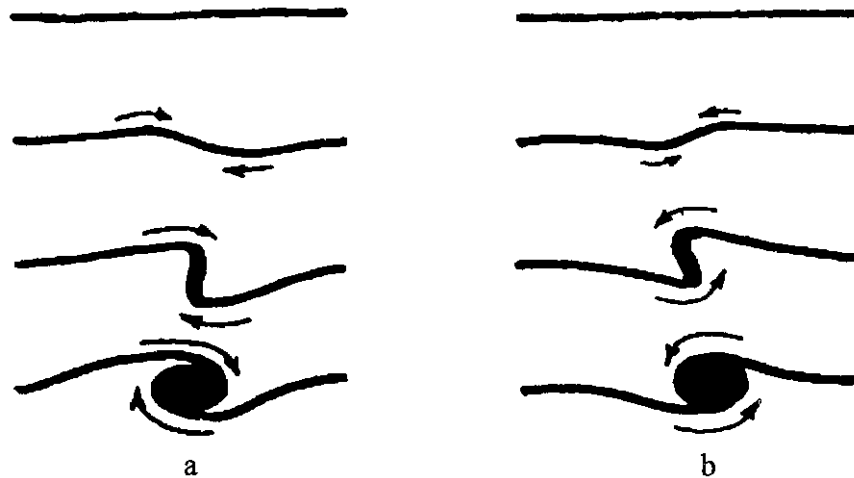
Figure 9. (a) Curl of trailing rotation as viewed from above in the northern hemisphere. (b) An arc structure having a rotational direction opposite to that in Figure 9(a) (after Oguti, 1974).

response to variations of solar wind parameters. This convection consists of two huge vortices of the Axford and Hines (1961) type and manifests itself in the polar ionosphere as the two-cell DP2-current system. This circulation may also be seen in the distribution and elongation of auroral arcs shown in Figure 8, after Davis (1962).

A classification scheme of relatively small-scale disturbed auroral structures was proposed by Akasofu and Kimball (1964). These authors distinguish such basic forms as rays, folds, loops (including so-called Ω-forms) and various combinations of them, and note that most of the above features are closely associated with specific motions of aurorae. In more detail, the relationship between auroral forms and their motions were studied by Hallinan and Davis (1970), Webster and Hallinan (1973), Oguti (1974), and summarized by Oguti (1975). According to the latter, the most important dynamic features are the rotation, folding and splitting of bright parts of aurorae.

So, Hallinan and Davis (1970) and Webster and Hallinan (1973) observed that *auroral rays* are often vortices which evolve out of thin sheets. These vortices (or curls in the terminology of Hallinan and Davis (1970)), which are approximately 2 km in diameter (the characteristic wavelength $\lambda \approx 5$ km according to Akasofu and Kimball (1964)) appear clockwise when viewed parallel to $\mathbf{B}$ (in this section, the sense of rotation is expressed as viewed from above the northern hemisphere). Development of such a curl is shown schematically in Figure 9(a), after Oguti (1974). Having compared Figure 9(a) with Table 2, one may identify such kind of features with the charge-sheet instability resulting from an excess of electrons within the sheet of precipitating particles (Webster and Hallinan, 1973).
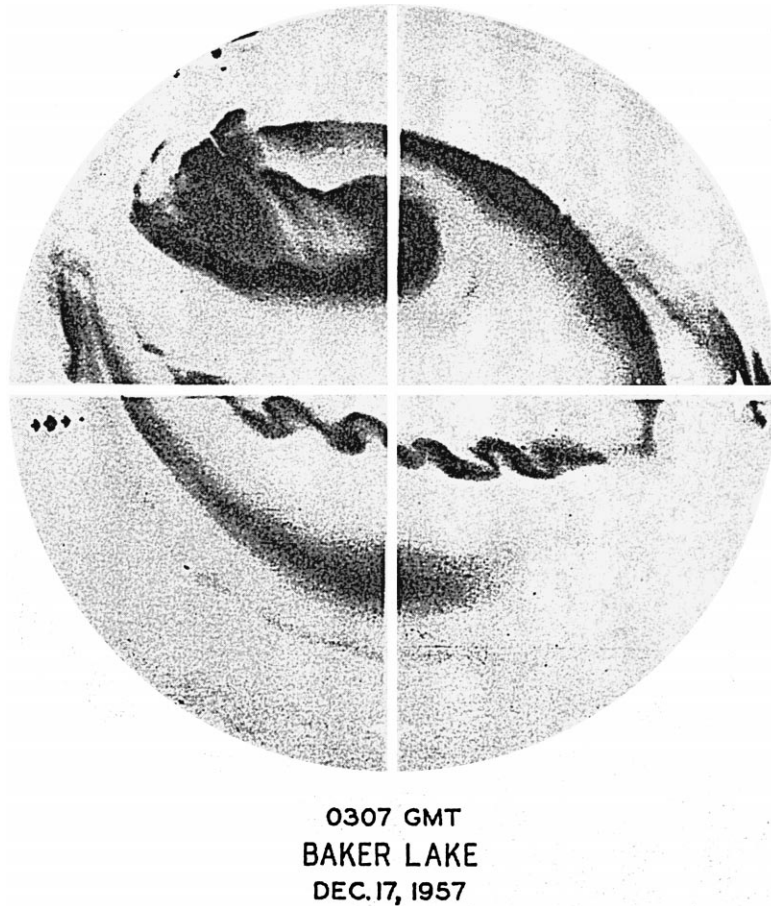
Figure 10. Small-scale folding structure recorded at Baker Lake at 03.07 hours GMT, 17 December, 1957 (after Akasofu and Kimball, 1964).

A feature to some extent similar to curls, is the 'trailing rotation' mentioned by Oguti (1974, 1975). It starts along an arc with some irregularities. Irregularities, a little brighter than the other parts, begin to rotate, and subsequently the rotating knots develop into a larger scale (Figure 10 after Akasofu and Kimball, 1964). This feature may be ascribed to the electron current-sheet instability.

According to Webster and Hallinan (1973), these sheets occur in groups, and a group as a whole can be treated as a single thicker sheet. This thicker sheet forms spirals or folds which can be from 30 to 1400 km in diameter (see Figure 11 after Akasofu and Kimball, 1964). Judging by their rotation sense, they are also caused by the electron current-sheet instability. The large spirals may evolve counterclockwise; then they are also examples of the electron current-sheet instability (Webster and Hallinan, 1973). However, according to Oguti (1974) counterclockwise rotational deformation, as shown in Figure 9(b), is very rare.
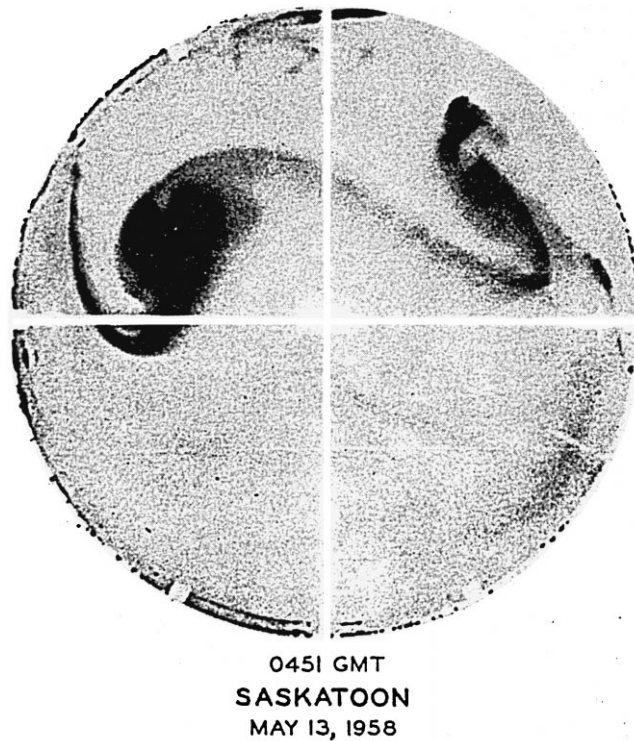
0451 GMT
SASKATOON
MAY 13, 1958

Figure 11. A large-scale 'crest' recorded at Baker Lake on 13 May, 1958, 04.51 GMT (after Akasofu and Kimball, 1964).

Another type of arc deformation is arc splitting (Oguti, 1974) resulting in the formation of S-structures (Oguti, 1975). S-type structures are very common features both in global and in local scales, especially in the dusk sector of the auroral zone. A fairly large S-structure is recognized as an auroral bulge or a westward traveling surge (WTS) (Akasofu et al., 1965; Oguti, 1975). In turn, the WTS may consist of smaller S-shaped folds, and there may be a considerable number of ray structures along the fold.

According to Oguti (1975), a typical S-structure is rotationally symmetric, which means that the forces producing the S-structure are also rotationally symmetric. Judging from the sense of rotation, these forces are produced by the excess of negative charge. The rotational velocity of auroral structures equals 5–8 km s^{-1} on average (Oguti, 1975), and sometimes reaches several tens of kilometers per second (Oguti, 1974), suggesting the transient appearance of a strong radial electric field in a small column extending above the active auroral display. The intensity of the equivalent electric field may exceed 1 V m^{-1} at the upper ionosphere level.

Nevertheless, counterclockwise rotation does take place in auroral motion, e.g., in the lower arm of the S-structure (Oguti, 1974), which suggests the existence
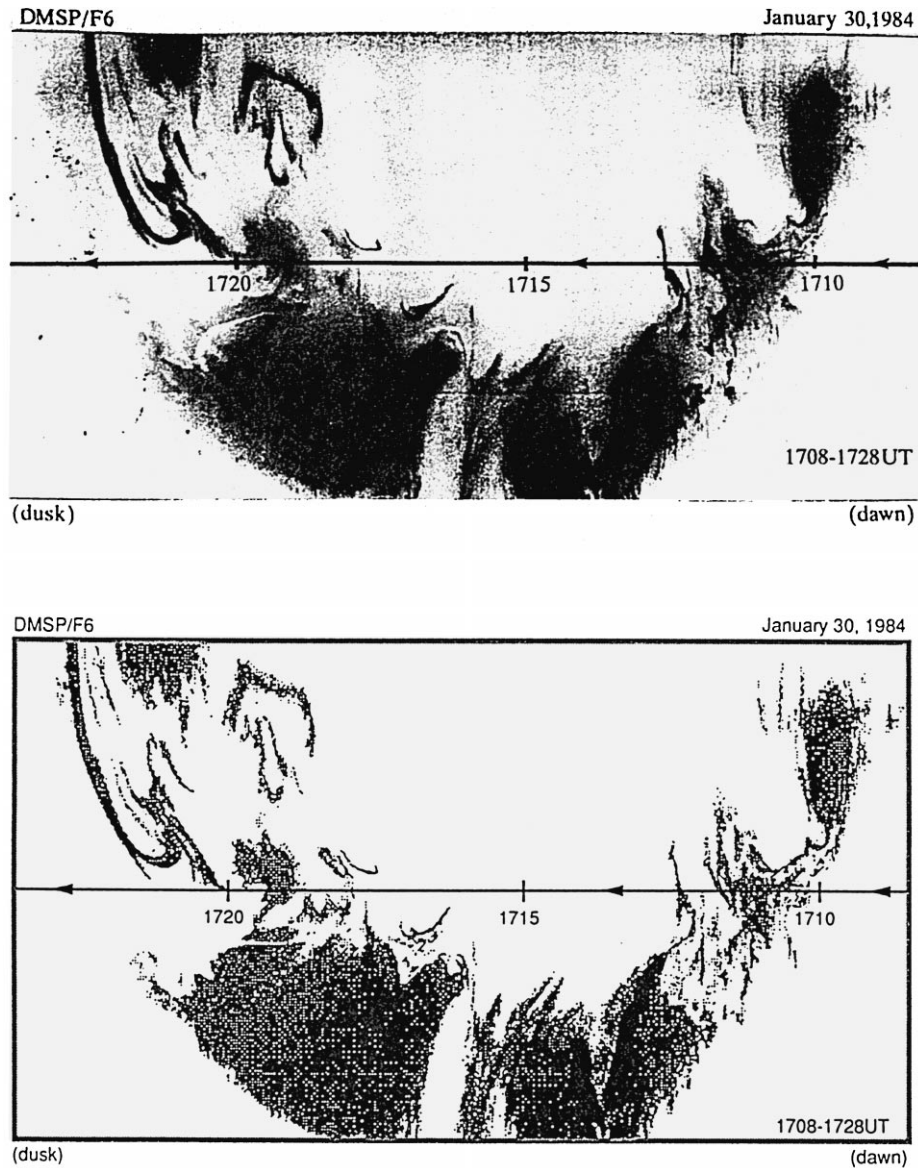
Figure 12. Omega bands and torch-like structures on the poleward boundaries of the diffuse aurora in the midnight-morning sector photographed from the DMSP-F6 satellite on 30 January, 1984 in the northern hemisphere (after Yamamoto et al., 1993).

there of a positive charge excess (see also Zaitseva, 1968). Thus, development of an *S*-structure seems to be associated with appearance of a dipole-like electric charge distribution, and hence with a pair of field-aligned currents.

One more type of large-scale folds in aurorae is the so-called Ω-bands (Akasofu and Kimball, 1964), and associated with them flame-structures (Oguti, 1975) and torches (Akasofu, 1974) (see Figure 12 after Yamamoto et al., 1993). Ω-bands (the characteristic wavelength of the disturbance is about 800 km (Lyons and Walterscheid, 1985)) occur preferably on the poleward boundary of the post-midnight diffuse aurora during the recovery phase of a substorm. The Ω-bands and torches drift eastward at velocities of 0.4–2 km s^{-1}. Saito (1978) has shown the Ω-bands to be associated with long-period geomagnetic pulsations. André and Baumjohann (1982) and Opgenoorth et al. (1983) have shown that Ω-bands are associated with a sequence of east-west oriented pairs of upward and downward directed field-aligned currents; the former flow from the bright tongue of the Ω-bands, and the latter into the dark hole.

The mechanism of generation of Ω-bands is not clear as yet. Rostoker and Samson (1984), Rajaram et al. (1986), Rostoker (1987), Connor and Rostoker (1993) proposed the Kelvin–Helmholtz instability developing at the boundary between the low-latitude boundary layer and the Central Plasma Sheet to be responsible for the generation of Ω-bands. On the other hand, Lyons and Walterscheid (1985) have supposed Ω-bands to be generated by shear instability of the neutral winds in the ionosphere. In this connection, the results reported by Steen et al. (1988) seem to be of some importance. According to their data, a distinct modulation of high-energy (>1 keV) particle intensity is observed at the geostationary orbit in an Ω-bands phenomenon, which suggests that torches–Ω-bands are of magnetospheric origin.

An attempt to develop a physical model of torches–Ω-bands was made by Yamamoto et al. (1993). We have to note, however, that the model in its present form seems to be erroneous. The fact is that in an isotropic and homogeneous plasma, the magnetic drift of particles is completely compensated by the diamagnetic current drift (Rossi and Olbert, 1970, Section 9.4), and magnetic-drift-induced instability can only take place in an anisotropic or inhomogeneous plasma. Thus, the model by Yamamoto seems to be in need of some corrections.

The global distributions of various auroral forms and of their motions are presented in Figures 13(a) and 13(b), respectively.

As is shown in these figures, in the dusk sector of the auroral zone, aurorae are observed in the form of thin arcs (current sheets with a negative charge excess) on the poleward edge of the auroral oval, and as diffuse arcs in the equatorward part of the latter. During the active phase of substorms, many clockwise vortices initiated by the splitting can develop along auroral arcs, so that the arc appears like a shear line of drifting auroral patches and arc fragments (see Figure 13(b)). The direction of the drift is eastward on the high-latitude side and westward on the low-latitude side of the arc, and the velocity of the drift can amount to 10 km s^{-1} on both sides (Oguti, 1974; Carlqvist and Bostrom, 1970) so that the equivalent electric field intensity may be ∼1 V m^{-1}.
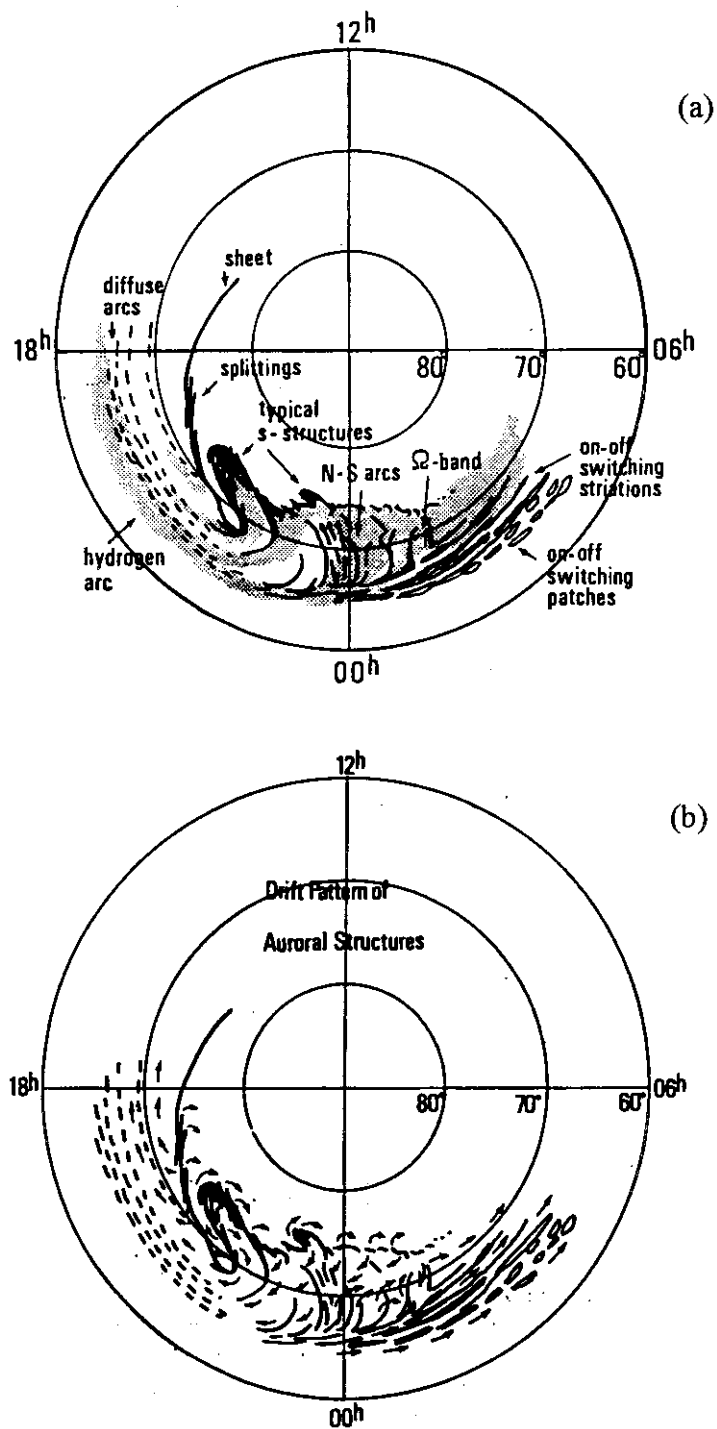
Figure 13. (a) Schematic distribution of aurorae and (b) schematic illustration of drifting patterns of auroral structures (after Oguti, 1975).

When an expansion occurs, S-structures appear in the evening sector of the auroral zone, which is recognized as a westward-travelling surge, and folds which expand poleward leaving behind many detached aurorae (Oguti, 1975).

In the midnight-morning sector there Ω-bands and torches are observed at the high-latitude boundary between the diffuse aurorae and the polar cap. As is seen from Figure 13(b), this boundary may also be considered as a shear line between the eastward flow on the high-latitude side of that line and the westward drift on the low-latitude side of it.

In the low-latitude part of the morning sector of the auroral zone, patchy aurorae are observed to move eastwards. Rostoker (1987) has attracted attention to the fact that aurorae of this kind also appear in the vicinity of a shear line separating eastward motion of discrete aurorae from anti-sunward motion of the plasma in the Low-Latitude Boundary Layer, which allows him to relate them (and associated Ps6 geomagnetic pulsations) to the development of the Kelvin–Helmholtz instability in the shear layer.

Similar phenomena seem to take place in the cusp region ionosphere, where specific traveling ionospheric vortices (TIV) are observed by radar backscattering (Southwood and Kivelson, 1993). These vortices have a horizontal scale of the order of 300–2000 km, and travel away from the noon meridian at speed about $1–5 \, \text{km s}^{-1}$. The nature of the disturbances is not clear as yet, and various physical mechanisms are proposed for their explanation (Miura, 1987; Pu et al., 1990; Southwood and Kivelson, 1993). In this connection, there attracts our attention the fact that the vortex system of TIV has a twin structure (Souhtwood and Kivelson, 1993), which allows us to suppose the disturbances under consideration to be associated with development at the magnetopause of some kind of the drift wave instability of the Hasegawa–Mima type.

Thus, in accordance with theoretical models, aurorae really display features associated with development of vorticity, and the variety of those features provides evidence of the variety of physical processes in the moving magnetospheric plasma. At the same time, we have to note that many concrete forms of auroral vorticity are not explained, and their relationship to certain plasma instabilities has not been found as yet. This especially concerns aurorae observed in the midnight sector of the auroral zone during the active phase of substorms. The variety of auroral forms and their motions at those periods are really astonishing; this seems to be associated with specific conditions in this region of the magnetosphere, characterized by the existence of intensive electric fields there, by sharp gradients of the plasma density and temperature, and by the influence of a relatively well-conducting and greatly inhomogeneous ionosphere. We believe that a detailed and thoughtful consideration of the auroral dynamics in this region would give us the key for understanding physical processes developing in the hot and inhomogeneous magnetospheric plasma, and thereby would allow us to discover the nature of magnetospheric substorms.

7. **Discussion**

As is seen from the experimental and theoretical data presented above, the characteristics of auroral vorticity are highly variable, and this variety is associated with the variety of physical mechanisms responsible for excitation of the plasma turbulence in the magnetospheric plasma. In turn, the diversity of these mechanisms is explained by the variety of physical conditions in various regions of the magnetosphere and the dependence on the intensity and the phase of magnetospheric disturbances. And though a universal theory of the auroral vorticity, which could explain all the variety of experimental data, does not exist as yet, one may state that:

(1) Magnetospheric plasma vorticity is transferred to the ionosphere by means of field-aligned currents, and the foci of convection vortices are associated with the existence of regions of electric space charge ($\nabla^2 \varphi \neq 0$).

This suggests that having obtained a 'snapshot' of auroral vorticity, it is possible to construct an instantaneous distribution of electrostatic potential in the ionosphere and in the magnetosphere. When the ionospheric conductivity is known (it may be calculated from the observations of the 3D distribution of the auroral luminosity), the distribution of field-aligned current intensity may be also calculated.

(2) The excitation of turbulence in a plasma flow is determined by the characteristics of that flow and, in particular, by the presence or absence of the primary vorticity within it; features of secondary vortices depend on the physical cause of the primary vorticity. Most often, the vorticity of the magnetospheric plasma flow is associated with the shear of the flow velocity; in turn, the velocity shear may be caused, as we have seen above, by gradients of the transverse electric field intensity, of the plasma density or temperature, and of the field-aligned current intensity. Characteristics of vortices excited by such sources may differ greatly in their shape (monopole- or dipole-like vortices in the case of ∇n and ∇T drifts (Laedke and Spatschek, 1986)), in the sense of the arm rotation (for charge or current sheets (Webster and Hallinan, 1973)), and in their size. This allows one to determine the physical mechanism of the turbulence excitation on the basis of observations of the characteristics of auroral vorticity.

(3) The power spectrum of observed vorticity also depends on the physical mechanism of the turbulence excitation. Thus, the spectral index k may vary from $k = -\frac{5}{3}$ for a current sheet instability (Seyler, 1990) to $k = -3$ for a drift wave instability with the kinematic ion viscosity taken into account (Haas, 1993), and to $k = -4$ for $\mathbf{E} \times \mathbf{B}$ drift shear instability (Miura and Sato, 1978).

This allows one to suppose that simultaneous observations of various characteristics of the auroral vorticity may provide one with sufficient information for distinguishing the mechanism of the turbulence excitation in any concrete situation under consideration.
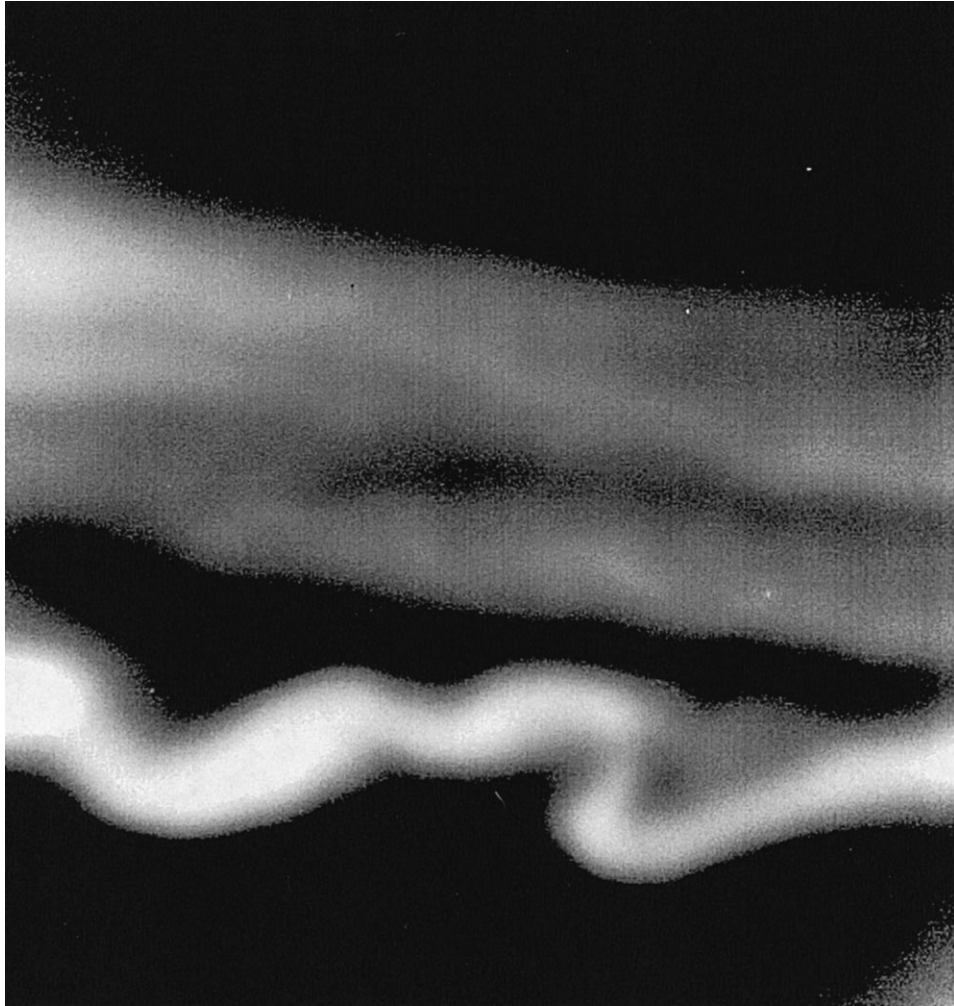
Figure 14a. ALIS auroral image data illustrating an example of vortex formation obtained from Kiruna station (wavelength 5577 Å, field of view 76 deg diagonal, integration time 1 s, north is up and east is left). A multiple auroral arc system on 7 April, 1995, 21:54:20 UT.

It seems worthwhile to discuss now what kind of observations need to be carried out to get information on the physical processes developing in the magnetospheric plasma.

(1) To obtain an instantaneous 3D-distribution of the auroral luminosity, it is necessary to have data of simultaneous observations of the auroral luminosity from a network of all-sky cameras. Then, using the methods of tomography, it would be possible to calculate the distribution of the auroral luminosity at any altitudinal level, and the energy spectrum of precipitated electrons. This would allow us to determine the location and the physical nature of the sources of auroral electrons.
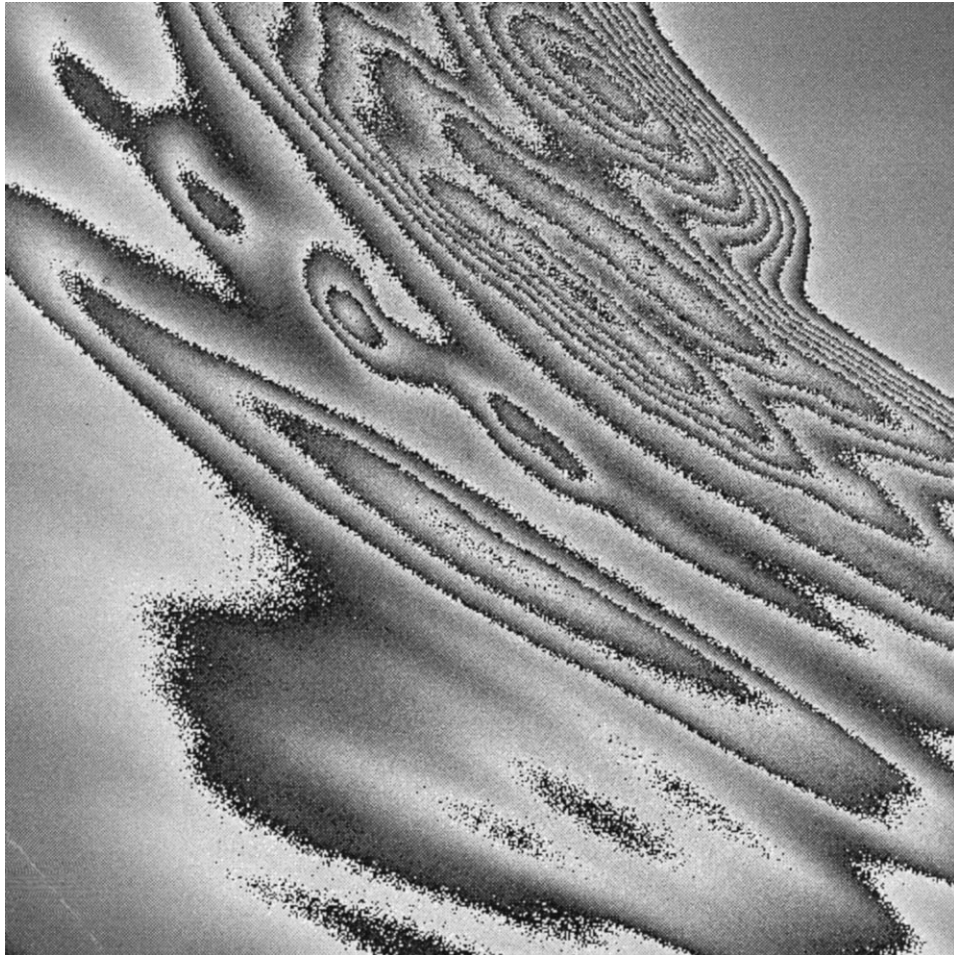
Figure 14b. ALIS auroral image data illustrating an example of vortex formation obtained from Kiruna station (wavelength 5577 Å, field of view 76 deg diagonal, integration time 1 s, north is up and east is left). Auroral iso-intensity contours for the same arc system.

(2) Analysis of all-sky films (visual or automatic) allows one to distinguish areas with curl-like, fold-like and other specific structures of aurorae. Then, having a series of successive all-sky films, it would be possible to calculate the 2D-distribution of the auroral velocity in those areas in order to trace the evolution of the vortices and of the vorticity, and to determine the sense of rotation of the auroral forms. Using these data, it would be possible to calculate the distribution of the electrostatic potential in the ionosphere and the field-aligned current intensity.

(3) Having the data on temporal variations of any parameter of the auroral vorticity (e.g., velocity of the auroral form motion, the intensity of auroral luminosity) one can construct the phase portrait of vorticity, its fractal dimension, and power spectrum.

Some of the observations outlined above can be carried out with ALIS, Auroral Large Imaging System (Steen and Brandstrom, 1996), a multi-station ground-based imaging system in northern Europe. ALIS auroral image data illustrating examples of vortex formation in auroral forms are given in Figure 14.

In Figure 14(a), a multiple auroral arc system on April 7, 1995, 20:38 UT is presented. One can see from the figure that the curled arc in the centre is a border between two regions, one of which is characterized by relatively quiet auroral arcs, and the second one is notable for greatly disturbed arcs with vortex structures.

In Figure 14(b), there are given iso-intensity contours for the same arc system. One can see from the figure that the curles in the central arc are developing predominantly clockwise (as seen from the ground), which corresponds, according to Table II, to the electron current instability, and the arc is most probably associated with an upward electric current sheet.

Future direction of work with ALIS includes fractal analysis of multi-station auroral images (Alpatov et al., 1996) and full 3-D reconstruction of specific auroral emissions (Gustavsson et al., 1996).

8. Conclusion

A short review of theoretical and experimental data on vorticity in the auroral form motion, presented above, shows that observations of the latter provides us with an abundant information on the physical state of the magnetospheric plasma and on the processes developing in it.

The complex of observations which are necessary for this information to be revealed is discussed, and a special system of auroral stations in the Northern Europe (ALIS) appropriate for this purpose is presented.

References

Akasofu, S.-I.: 1966, *Sci. Amer.* **213**, 6, 55.
Akasofu, S.-I.: 1974, 'A Study of Auroral Displays Photographed from DMSP-2 Satellite and from the Alaska Meridian Chain of Station', preprint, Geophys. Res. Inst., Univ. of Alaska.
Akasofu, S.-I. and Kimball, D. S.: 1964, *J. Atmospheric Terrest. Phys.* **26**, 205–211.
Akasofu, S.-I., Kimball, D. S., and Meng, C.-I.: 1965, *J. Atmospheric Terrest. Phys.* **27**, 189.
Alpatov, V., Steen, A., Brandstom, U., and Gustavsson, B.: 1996, 'Fractal Analysis of the ALIS Auroral Images', *Geophys. Res. Lett.*, submitted.
André, D. and Baumjohann, W.: 1982, *J. Geophys. Res.* **50**, 194–201.
Axford, W. J. and Hines, C. O.: 1961, *Can. J. Phys.* **39** (10), 1433–1464.
Batchelor, G. K.: 1970, *An Introduction to Fluid Dynamics*, Cambridge University Press, Cambridge.
Beer, T.: 1974, *Atmospheric Waves*, Adam Hilger Ltd, London.
Carlqvist, P. and Boström, R.: 1970, *J. Geophys. Res.* **75**, 7140–7146.
Chamberlain, J. W.: 1961, *Physics of the Aurora and Airglow*, Academic Press, New York.
Connors, M. and Rostoker, G.: 1993, *Geophys. Res. Lett.* **20** (15), 1535–1538.
Davis, T. N.: 1962, *J. Geophys. Res.* **67** (1), 75–110.
Dungey, J. W.: 1958, *Cosmic Electrodynamics*, Cambridge University Press, Cambridge.

Evans, D. S.: 1974, *J. Geophys. Res.* **79**, 2853–2858.

Evans, D. S.: 1975, *Physics of Hot Plasma in the Magnetosphere*, Plenum Press, New York.

Fleagle, R. G. and Businger, J. A.: 1980, in J. Van Mughem and A. L. Hales (eds.), *Atmospheric Physics, Int. Geophys. Series* **25**.

Gustavsson, B., Brandstom, U., and Steen, A.: 1996, 'ALIS Tomographic Results', *J. Geophys. Res.*, submitted.

Haas, F. A.: 1993, in T. O. Dendy (ed.), *Plasma Physics: An Introductory Course*, Cambridge University Press, Cambridge, pp. 103–128.

Hallinan, T. J.: 1976, *J. Geophys. Res.* **81** (22), 3959–3965.

Hallinan, T. J. and Davis, T. N.: 1970, *Planetary Space Sci.* **18**, 1735–1744.

Hasegawa, A.: 1970, *Phys. Rev. Lett.* **24** (21), 1162–1165.

Hasegawa, A. and Sato, T.: 1989, *Space Plasma Physics*, Section 2.9, Springer-Verlag, Berlin.

Holton, J. R.: 1992, *An introduction to Dynamics Meteorology*, Academic Press, New York.

Karlson, E. T.: 1962, *Phys. Fluids* **5**, 476–486.

Laedke, E. W. and Spatschek, K. H.: 1986, *Phys. Fluids* **29** (1), 133–142.

Liperovsky, V. A. and Pudovkin, M. I.: 1983, *Anomalous Resistivity and Double Layers in the Magnetospheric Plasma*, Nauka, Moscow (in Russian).

Lyons, L. R. and Walterscheid, R. L.: 1985, *J. Geophys. Res.* **90** (12), 12321–12329.

Miura, A.: 1987, *J. Geophys. Res.* **92**, 3195.

Miura, A. and Sato, T.: 1978, *J. Geophys. Res.* **83** (A5), 2109–2117.

Oguti, T.: 1974, *J. Geophys. Res.* **79** (25), 3861–3865.

Oguti, T.: 1975, *Mem. Nat. Inst. Polar Res. Sec. A* (12), pp. 1–101.

Opgenoorth, H. J., Oksman, J., Kaila, K. U., Nielsen, E., and Baumjohann, W.: 1983, *J. Geophys. Res.* **88**, 9171–9185.

Petviashvili, V. I.: 1977, *Soviet Plasma Phys.* **3** (2), 270–276 (in Russian).

Pu, Z. Y., Yei, M., and Lin, Z. X.: 1990, *J. Geophys. Res.* **95**, 10559.

Pudovkin. M. I., Shumilov, O. I., and Zaitseva, S. A.: 1968, *Planetary Space Sci.* **16**, 881–890.

Rajaram, G., Rostoker, G., and Samson, J. C.: 1986, *Planetary Space Sci.* **34** (3), 319–329.

Rossi, B. and Olbert, S.: 1970, *Introduction to the Physics of Space*, McGraw-Hill, New York.

Rostoker, G. and Samson, J. C.: 1984, *Geophys. Res. Lett.* **11** (3), 271–274.

Saito, T.: 1978, *Space Sci. Rev.* **21**, 427–467.

Seyler, C.: 1990, *J. Geophys. Res.* **95** (A10), 17199–17215.

Southwood, D. J. and Kivelson, M. G.: 1993, *J. Geophys. Res.* **98** (A7), 11459–11466.

Spatschek, K. H. and Laedke, E. W.: 1986, in T. D. Guyenne and L. M. Zeleny eds), *Proceedings of the Joint Varenna-Abastumany International School and Workshop*, ESA Publ. Div., pp. 61–68.

Steen, A., Collis, P. N., Evans, D., Kremser, G., Kapelle, S., Rees, D., and Tsurutani, T.: 1988, *J. Geophys. Res.* **93**, 8713–8733.

Steen, A. and Brandstom, U.: 1996, 'ALIS – Versatile Multi-Station Imaging System at High Latitudes', *J. Geophys. Res.*, submitted.

Walker, A. D. M.: 1981, *Planetary Space Sci.* **29** (10,) 1119–1133.

Webster, H. F. and Hallinan, T. J.: 1973, *Radio Sci.* **8** (5), 475–482.

Yamamoto, T., Makita, K., Ozaki, M., and Meng, C.-I.: 1993, *J. Geomagn. Geoelectr.* **45**, 619–648.

Yu, M. Y. and Lisak, M.: 1986, *Phys. Fluids* **29** (1), 143–145.

Zaitseva, S. A.: 1968, in S. I. Isaev and Ya. I. Feldstein (eds.), *Aurora*, Nauka, Moscow, pp. 34–38.